

# Seismic Analysis of the LSST Telescope

Douglas R Neill<sup>a</sup>

<sup>a</sup>National Optical Astronomy Observatory, 950 N. Cherry, Tucson, AZ, USA 85719

## ABSTRACT

The Large Synoptic Survey Telescope (LSST) will be located on the seismically active Chilean mountain of Cerro Pachón. The accelerations resulting from seismic events produce the most demanding load cases the telescope and its components must withstand. Seismic ground accelerations were applied to a comprehensive finite element analysis (FEA) model which included the telescope, its pier and the mountain top. Response accelerations for specific critical components (camera and secondary mirror assembly) on the telescope were determined by applying seismic accelerations in the form of Power Spectral Densities (PSD) to the FEA model. The PSDs were chosen based on the components design lives. Survival level accelerations were determined utilizing PSDs for seismic events with return periods 10 times the telescope's design life which is equivalent to a 10% chance of occurring over the lifetime. Since the telescope has a design life of 30 years it was analyzed for a return period of 300 years. Operational level seismic accelerations were determined using return periods of 5 times the lifetimes. Since the seismic accelerations provided by the Chilean design codes were provided in the form of Peak Spectral Accelerations (PSA), a method to convert between the two forms was developed. The accelerations are also affected by damping level. The LSST incorporates added damping to meet its rapid slew and settle requirements. This added damping also reduces the components' seismic accelerations. The analysis was repeated for the telescope horizon and zenith pointing. Closed form solutions were utilized to verify the results.

**Keywords:** telescope, earthquake, seismic, accelerations, PSD, PSA

## 1. INTRODUCTION

The LSST will be built on a 2,682 meter high mountain, Cerro Pachón, Chile. This location is seismically active, consequently the telescope (and all its components) must be designed to withstand the potential seismic accelerations. These seismic accelerations are the most demanding load cases the telescope must be designed to withstand. As a result of their locations, figure 1, the components expected to experience the highest accelerations are the camera and secondary mirror assembly. They are also significantly susceptible to seismic damage. Consequently, these components are the focus of this analysis.

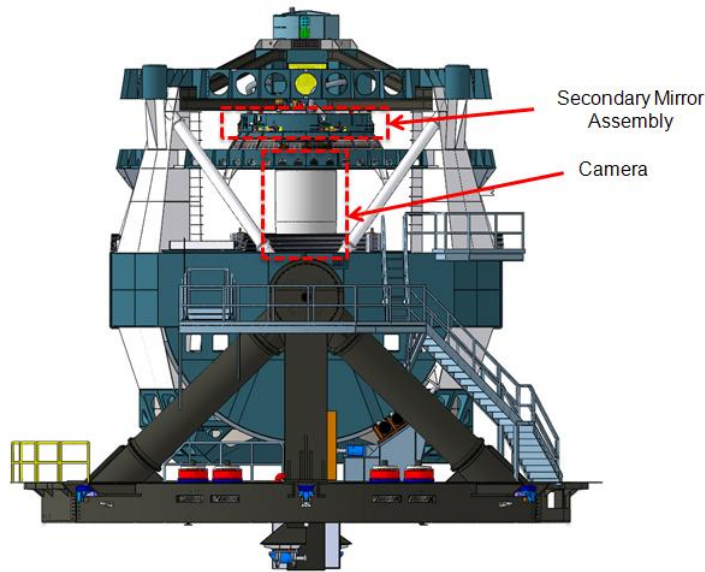


Figure 1. LSST Telescope: Secondary Mirror Assembly and Camera locations.

In the companion document<sup>[1]</sup>, "Seismic Design Accelerations for the LSST Telescope," the expected seismic accelerations were determined in the form of Peak Spectral Accelerations (PSA) based on the Chilean Standard<sup>[2]</sup> (Norma Chilena), "Earthquake - Resistant design of base-isolated buildings." Although this design standard is intended for base isolated buildings, it provides the most detailed peak spectral accelerations of any of the relevant Chilean Standards. The other Chilean Standards<sup>[3,4]</sup> are not directed toward seismically isolated buildings. The natural frequencies of these structures are not accurately determined and therefore detailed PSAs are not provided.

In the companion document<sup>[1]</sup>, the ground accelerations were determined in the form of PSAs, figure 2. Although this is the commonly utilized format for seismic accelerations it is uncommon in most types of vibration analysis. It cannot be directly applied in a finite element analysis (FEA) to determine the propagation of accelerations throughout the telescope mount, and the resulting component accelerations. Since a PSA provides the accelerations for a single degree of freedom damped resonator to a seismic ground motion, it has both damping and amplification information embedded in it. Consequently, the PSA must first be converted to a Power Spectral Density (PSD) before it can be utilized in an FEA analysis.

Most commonly, seismic analysis of a building is conducted using the accelerations corresponding to a 500 year seismic event<sup>[3]</sup>. This is an event with an average 500 year return period and is equivalent to a 20% chance over 100 years or a 10% chance over 50 years. A building can easily last for 50 years and seismic damage to a building also endangers personnel, consequently a 500 year event (10% chance over 50 years) provides reasonable design accelerations for occupied buildings.

Limited lifetime equipment, such as a telescope, should be designed to seismic accelerations reflecting their design lifetimes. Following the previous example of buildings implies that the LSST telescopes with its 30 year design life should be designed to survive a 300 year seismic event.

The 300 year seismic event provides the "survival level" accelerations for the telescope, its mount and all its components. Survival implies that no catastrophic, ultimate failures, or cascading failures occur. However, a significant level of damage is expected. Although some components, the camera for example, have shorter design lifetimes than the telescope mount, they are required to survive the same 300 year seismic event. Otherwise, their failures could produce cascading failures to other components with longer lifetimes. Besides the survival level event, all components must be designed for an "operational level" event. After an operational level event, no appreciable damage is allowed. The component must remain operational with some minor exceptions regarding calibration, etc. The operational level events have been set to a 20% probability during the lifetime of the telescope. For the telescope mount and the secondary mirror assembly this implies a 150 year return seismic event for its operational level. The camera's 15 year design life corresponds to a 75 year return event.

Although the seismic accelerations were determined from the Chilean Standard<sup>[2]</sup>, "Earthquake - Resistant design of base-isolated buildings," the actual analysis was conducted utilizing the guidelines of the Chilean Standard<sup>[3]</sup>, "Seismic design for industrial structures and facilities." This reference<sup>[3]</sup> is intended for industrial structures similar to the LSST telescope.

- Separate analyses were conducted for accelerations in two orthogonal horizontal directions (X, Y)
- The two horizontal results were combined RSS with results for the vertical direction (Z) but not with each other.
- Only spectral analysis accelerations were utilized and not time domain accelerations.
- Only linear analysis was performed.

## **2. PSA: PEAK SPECTRAL ACCELERATIONS**

The expected accelerations produced by a seismic event are most often provided in the form of a Peak Spectral Acceleration (PSA) plot. The PSA can be used to provide either horizontal or vertical accelerations. The PSA provides the response (output) accelerations for a single degree of freedom resonator. The response is the result of the interaction of the ground acceleration and the amplification resulting from the dynamic properties of a structure, figure 2.

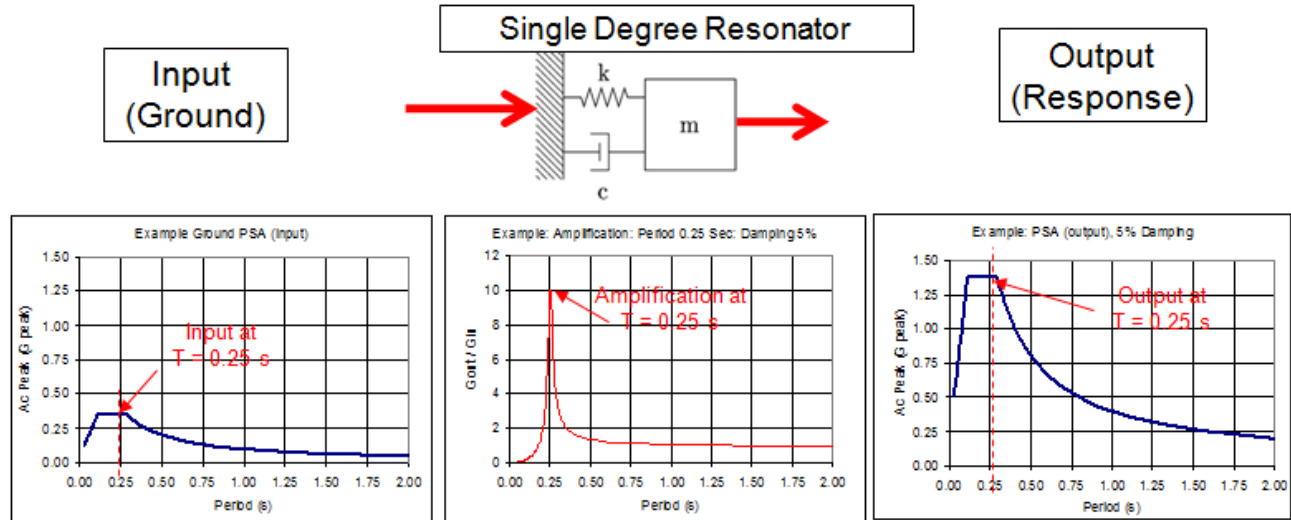


Figure 2. Illustration of PSA determination (Note: This is a simplification for explanation purposes).

The PSA is normally plotted with the peak acceleration ( $A_c$  peak) in gravitational units (G peak) versus the fundamental period (inverse of natural frequency) in seconds (s). The PSAs determined through [1] and utilized in this analysis are shown in figure 3. The 300 year return event corresponds to the survival design accelerations for all the telescope (mount) and all the components, the 150 year return events corresponds to the operational level accelerations for the mount and the secondary mirror assembly and the 75 year return event corresponds to the operational level accelerations of the camera.

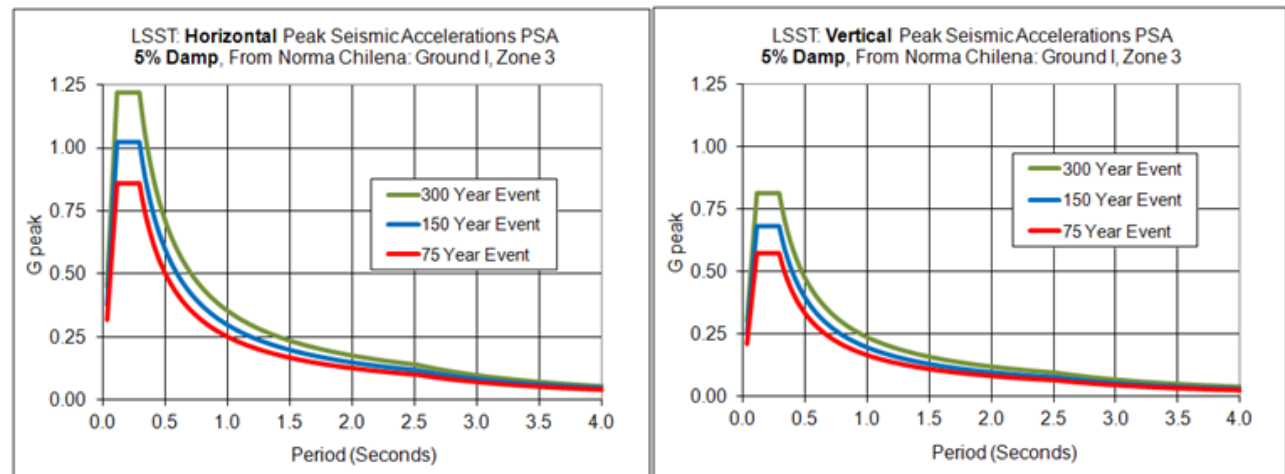


Figure 3. LSST Horizontal and Vertical Design PSAs.

If the natural frequency of a structure is known then the peak seismic acceleration can be read directly off of the PSA. For example, from figure 3, for a 300 year event, the peak accelerations for a 8 Hz (0.125 s) natural frequency resonator is 1.2 G horizontal and 0.8 G vertical. This is essentially the accelerations of the CG of the telescope mount and could be used directly for determining the seismic loading between the telescope mount and its foundation. However, there is a substantial variation in acceleration throughout the telescope.

Both the camera and secondary mirror assembly are supported and positioned by hexapods. The legs of these hexapods function as stiff springs. The lowest vibration modes of the camera (or secondary mirror assembly) result from deformation of these hexapods. The presence of the telescope mount between the ground acceleration and the hexapod bases substantially modifies the dynamic input to these two components. The camera does not experience the ground acceleration, but instead the output accelerations resulting from the interaction of the ground acceleration and the

telescope's dynamics. This interaction is a function of the natural frequencies of the telescope and the camera on its hexapod, the damping level and the spectrum of the input ground accelerations. In general, this interaction increases the acceleration of the camera (or secondary mirror assembly).

### 3. POWER SPECTRAL DENSITY (PSD)

Other than for presenting seismic responses, the most common curve used in vibration analysis is the PSD, Power Spectral Density (P). The PSDs shown in figure 4 are equivalent to the PSAs shown in figure 3. Although the PSD is more cumbersome than the PSA it is more useful since it can be accurately utilized to determine the coupling induced accelerations of individual components through finite element analysis and other numerical methods.

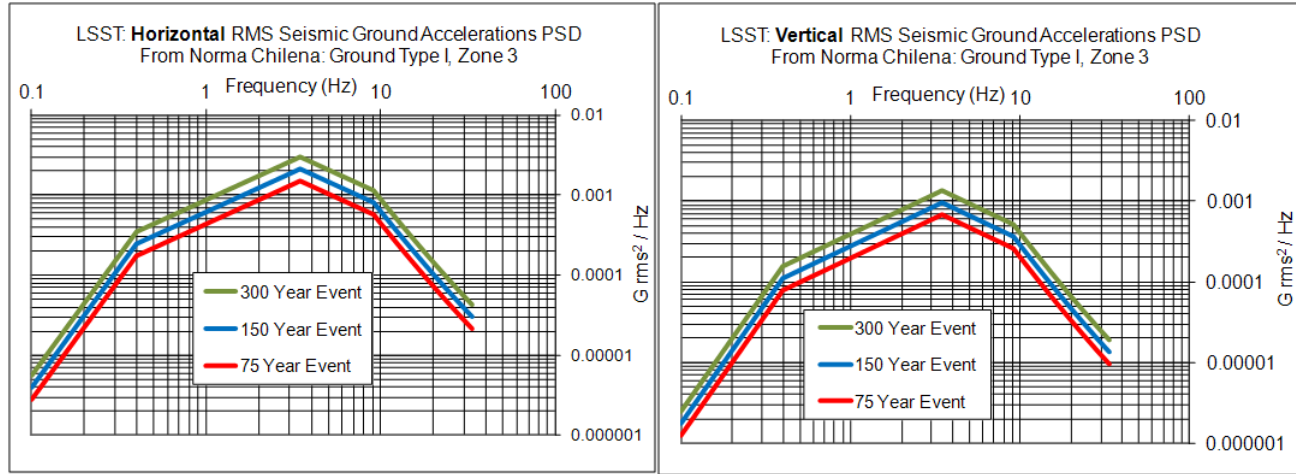


Figure 4. LSST Horizontal and Vertical Design PSDs.

The PSD commonly plots the log of (P) in  $G \text{ rms}^2 / \text{Hz}$  versus the log of frequency (f) in Hz. The accelerations ( $A_c$ ) produced by a single degree of freedom resonator and for a single vibration frequency can be determined by multiplying the value of P at a specific frequency, by that frequency and then taking the square root. For example, the horizontal accelerations at 10Hz and for a 300 year event:

- $P = 0.001 G \text{ rms}^2 / \text{Hz}$
- $P * f = 0.001 G \text{ rms}^2 / \text{Hz} * 10 \text{ Hz}$
- $A_c = (P * f)^{1/2}$   
= 0.10 G rms

An output PSD (response) can be determined by combining an input PSD with the resonator's amplification. The input PSD value ( $P_{in}$ ) for each frequency is multiplied by the square of the amplification ( $A^2(f)$ ) at that frequency to determine the value of the output PSD ( $P_{out}$ ) at that same frequency, figure 5.  $P_{out}(f) = A^2(f) * P_{in}(f)$ , where  $P_{out}$  and  $P_{in}$  are curves on their respective PSDs and not single values. The amplification (A) is the ratio of the output acceleration to the input acceleration. Although, in general, real structures have complicated amplifications for a simple single degree of freedom isolator the amplification can be calculated by[5]:

$$A = \frac{1}{2R\sqrt{1 - (f/f_n)^2}}$$

Where:

- $f$  = frequency;
- $f_n$  = natural frequency;
- $R$  = damping (e.g.  $R = 0.05$  for 5% damping).

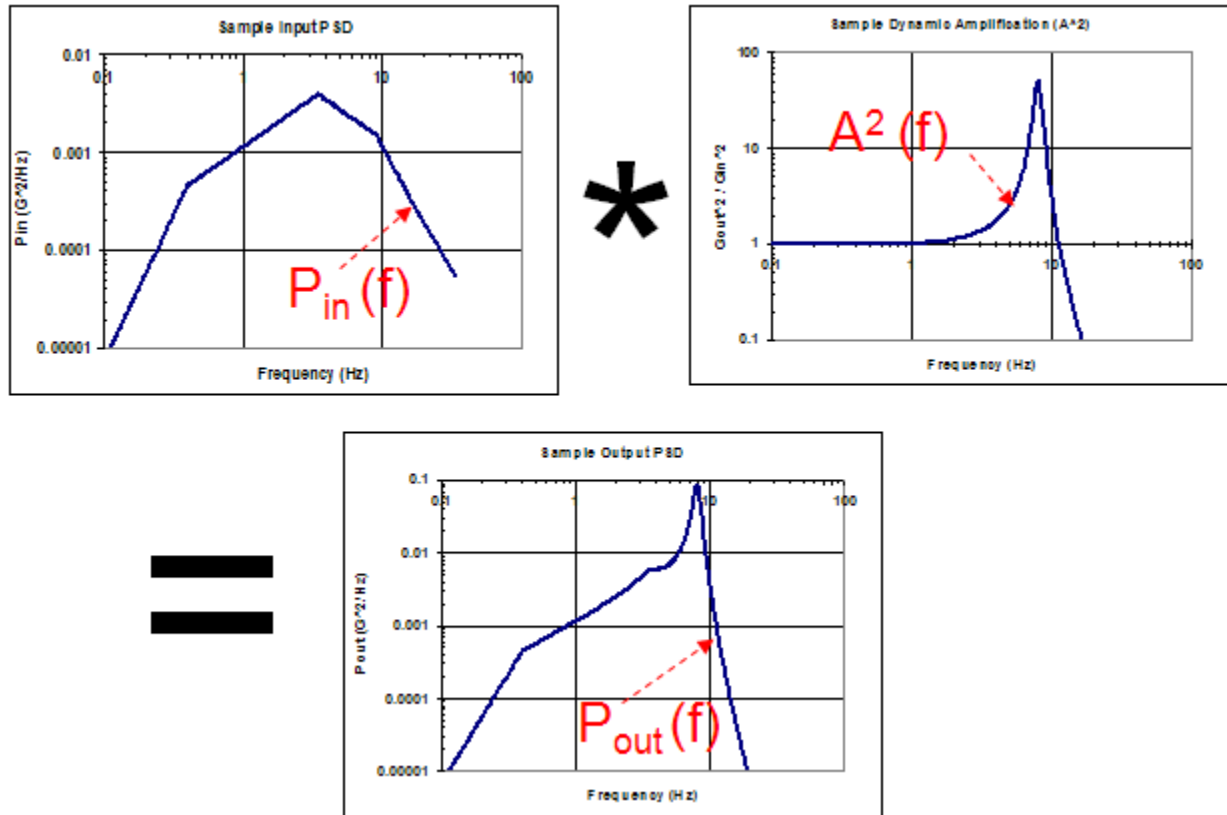


Figure 5. Determination of output PSD from input PSD and amplification of an 8 Hz resonator.

The total RMS acceleration ( $A_{c rms}$ ) can be computed from a PSD by integrating  $P$  (the value plotted on the PSD in  $G_{rms}^2/Hz$ ) over the PSD's frequency range. This integration can be presented graphically in an integrated response plot, figure 6. The RMS acceleration ( $A_{c rms}$ ) is then the square root of this integrated value. Statistically, from [5] page 204, the Peak acceleration ( $A_{c Peak}$ ) is three times the rms acceleration ( $A_{c rms}$ ), [ $A_{c Peak} = 3 \times A_{c rms}$ ]. This relationship is for either an input or output PSD.

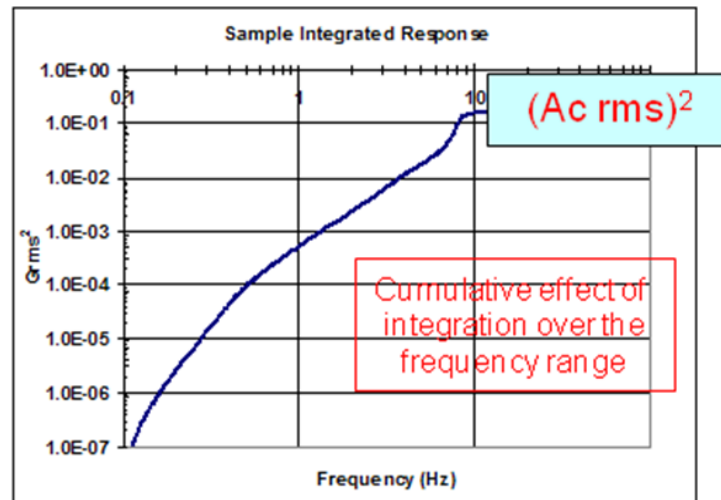


Figure 6. Determination of total acceleration from integrating a PSD

The peak acceleration determined by the method above from a PSD only corresponds to a single point on the PSA where the period on the PSA corresponds to the fundamental natural frequency of the single degree of freedom resonator amplification utilized by the PSD. Producing an entire PSA from a PSD using the above method requires repeating the above steps for every individual fundamental period (natural frequency) on the entire plot.

#### 4. SIMPLIFIED PSD AND PSA RELATIONSHIP

There are significant differences between the PSD and the PSA. The acceleration from the PSA is the peak acceleration for a single resonator (structure), versus the fundamental period (inverse of natural frequency  $f_n$ ) of that resonator. Each point on the plot represents the peak acceleration of a different resonator at its own natural frequency. The accelerations on a PSD are typically the rms (root-mean-square) accelerations for each vibration frequency. All of the vibrations represented by the PSD are assumed to occur simultaneously. The accelerations represented are for a single resonator at its own natural frequency or for the ground. Consequently the peak acceleration is a function of the entire curve. Although the PSA is principally used for presenting outputs (responses), the PSD is used equally for both inputs and outputs.

The previous mathematically exact relationship described between the PSD and PSA is cumbersome and difficult to use for converting from a PSD to a PSA. Since the exact conversion from the PSD to the PSA involves an integration, there are an infinite number of PSDs that when integrated will match any point on the PSA. Consequently, there is no mathematically exact method to convert a PSA to a PSD. Fortunately there is a relatively simple conversion between the two when the PSD is broad band (white noise) [5], page 207, figure 7.

- $Ac_{rms} = \sqrt{(\pi/2) P_{in} f_n Q}$  or  $P_{in} = (Ac_{rms})^2 / ((\pi/2) f_n Q)$ 
  - $f_n$  = natural frequency
  - $P_{in}$  = Constant broad band PSD value
  - $Q = 1 / \{2 * R\}$  where R is the damping
- $Ac_{Peak} (PSA \text{ value}) = 3 * Ac_{rms} (PSD \text{ determined value})$
- $Ac_{peak} = 3 * \sqrt{(\pi/2) P_{in} f_n Q}$  or  $P_{in} = (Ac_{peak}/3)^2 / ((\pi/2) f_n Q)$

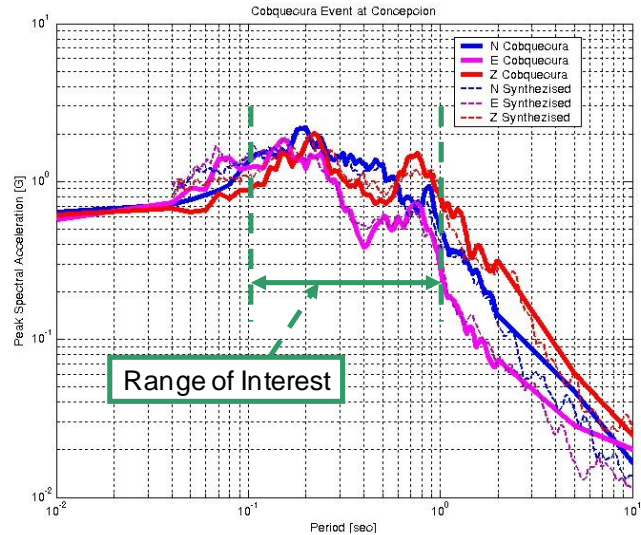
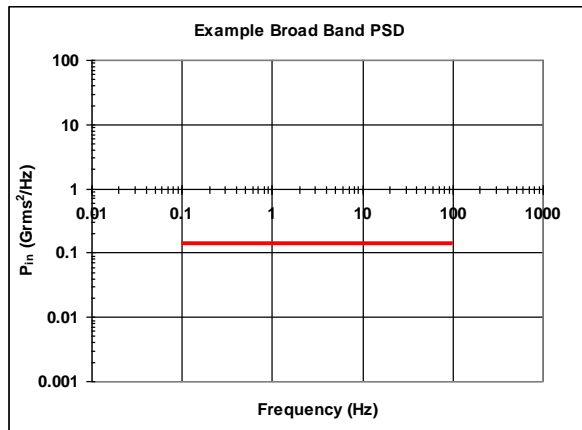


Figure 7. Example of Broad Band (constant  $P_{in}$ ) PSD and Actual Seismic PSD

The previous equation was produced by integrating the product of a constant value of  $P_{in}$  and the amplification equation. Although it was developed for a constant value it can be utilized for a more realistic  $P_{in}$  which is a function of frequency. This equation assumes that most of the acceleration is produced by vibrations at the natural frequency. Consequently, when the natural frequency ( $f_n$ ) is near the maximum value on the PSD curve, the equation will produce an accurate and slightly conservative estimate of the actual peak acceleration. When the natural frequency is not near the maximum value on the PSD curve, the equation can produce non trivial errors. Over the range of interest ( $1 < f_n < 10$ ) for



astronomical telescopes, earthquakes are reasonably broad band and the peak values of the PSD are near these frequencies. Consequently, the simplified equation presented earlier is valid.

The accuracy of this method for converting between PSD and PSA was demonstrated by manipulating real data. Measured seismic ground accelerations were used. The PSD for these accelerations was determined. The PSD was converted into a PSA using mathematically exact methods. The PSA was converted back into a PSD using the simplified equation. The new PSD and the original PSD were nearly identical.

## 5. ANALYSIS

Utilizing FEMAP NASTRAN software a comprehensive FEA model was developed of the LSST telescope mount, its pier and the mountain top, figure 8. The 300 year seismic PSDs were applied to determine the accelerations of the camera and the secondary mirror system through a 4 step process. 1) The natural frequencies of the FEA model, figure 9, were determined. 2) The amplifications, figure 10, were determined in the form of frequency responses for constant 1G peak magnitude sinusoidal input ground accelerations. 3) The input seismic ground PSDs were combined in post processing with the amplifications (frequency responses) to determine the output (response PSD), figure 11, of the secondary mirror assembly and camera. 4) The output PSDs were integrated over frequency to determine the RMS accelerations and finally the peak acceleration by multiplying by 3.

Separate responses were determined for all three azimuth assembly coordinate directions (X, Y, Z), figure 8. The X axis is along the telescope's elevation axis, the Z axis is vertical positive up and the Y axis is determined by the right hand rule.

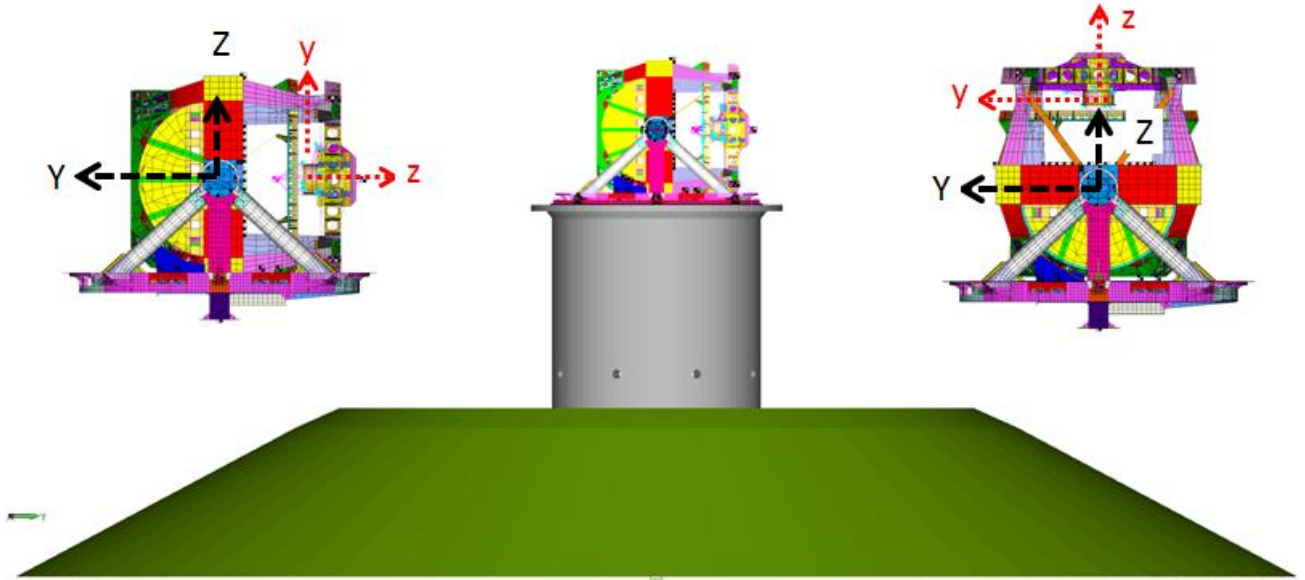
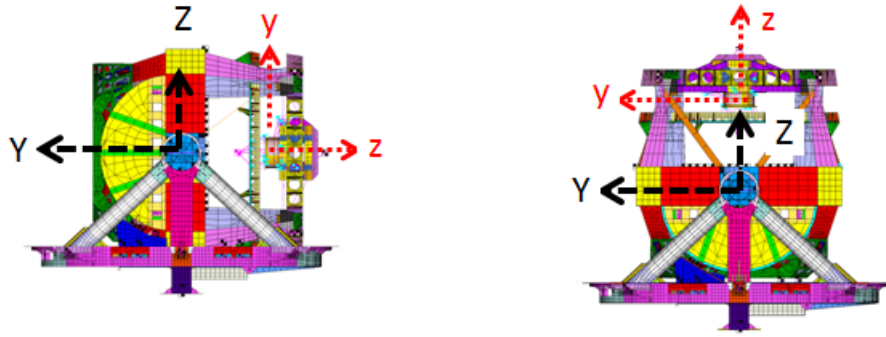


Figure 8. Coordinate Systems and Comprehensive FEA model of telescope, Pier and Mountain Top.



Horizon Pointing: Vibration Modes			Vertical Pointing: Vibration Modes		
Mode #	Frequency (Hz)	Mode Shape	Mode #	Frequency (Hz)	Mode Shape
1	7.53	Telescope X Translation	1	7.51	Telescope X Translation
2	8.38	Telescope Y Trans / X Rot	2	8.86	Telescope Y Trans / X Rot
3	11.37	Telescope Z Translation	3	11.36	Telescope Z Translation
4	11.68	Camera X (x) Translation	4	11.71	Camera X (x) Translation
5	12.55	Camera Y (z) Translation	5	12.40	Camera Z (z) Translation
6	13.99	Camera X (x) Rotation	6	13.34	Camera Y (y) Translation
7	14.74	Telescope Z Rotation	7	14.70	Camera Y (y) Rotation
8	15.83	Camera Y (z) Translation	8	15.37	Telescope Z Rotation
9	15.87	Camera Y (z) Translation	9	15.98	Camera Z (z) Translation
10	16.58	Camera X (x) Rotation	10	16.32	Camera X (x) Translation

Figure 9. Natural Frequencies of LSST telescope.

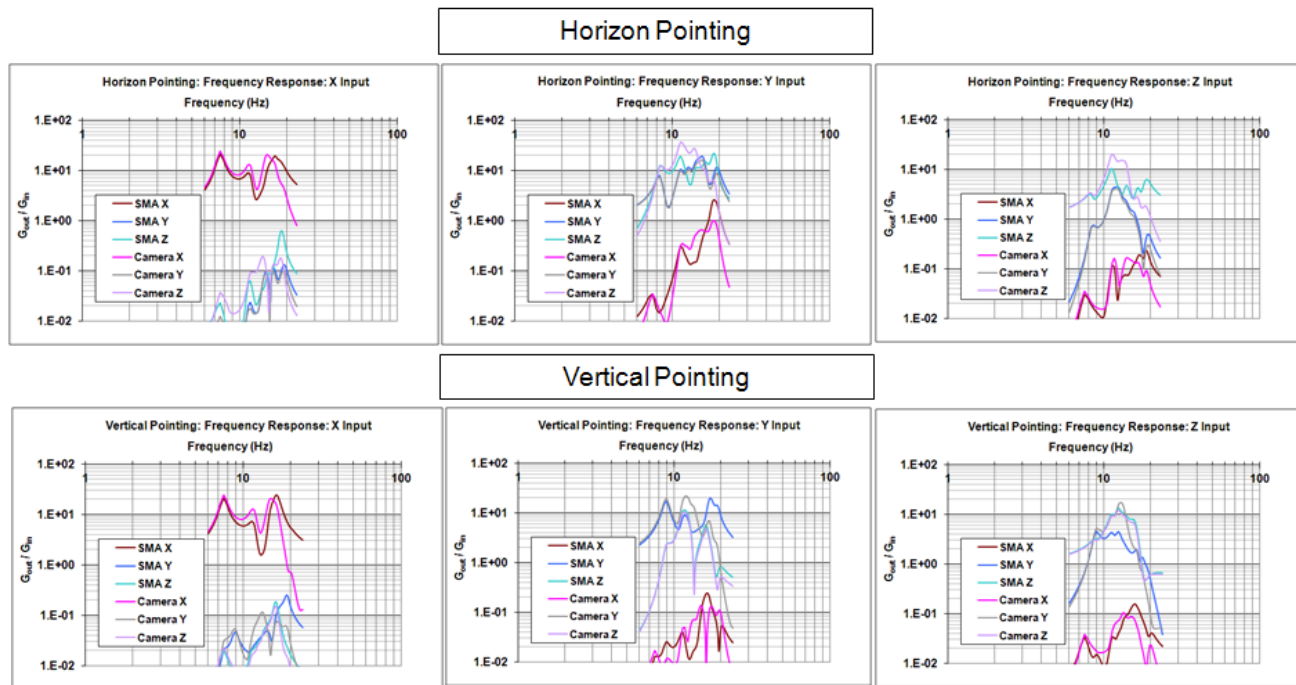


Figure 10. Amplifications (1 G unit acceleration frequency responses) of secondary mirror assembly and camera.

This initial analysis was only conducted for the telescope horizon pointing and zenith pointing. Since the total acceleration is a combination of seismic and gravitational accelerations, the worst case overall loading is expected to be near these orientations. The LSST elevation assembly also has a unique property of nearly equal moments of inertia in all



three directions. Consequently, minimal variation of response with elevation angle is expected. For completeness an intermediate angle will be included in the final analysis however, this has not been conducted at the time of this report.

For each input acceleration PSDs (X, Y *or* Z) the output PSD, in all three directions (X, Y *and* Z), was determined directly by the FEA analysis software, figure 11. These output PSDs were exported to the Microsoft EXCEL software and integrated over frequencies. As discussed earlier, the rms accelerations equals the square root of this integrated value and the peak acceleration is 3x the rms acceleration, figure 12, table 1.

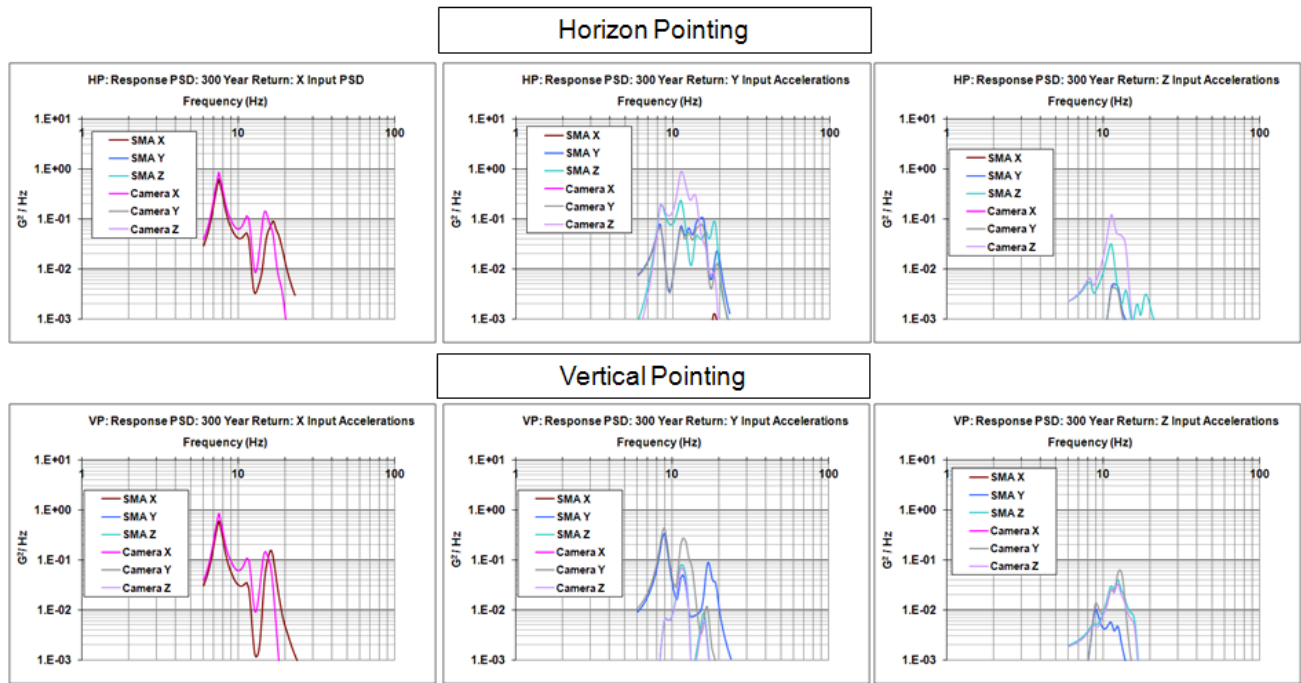


Figure 11. Seismic Output PSDs

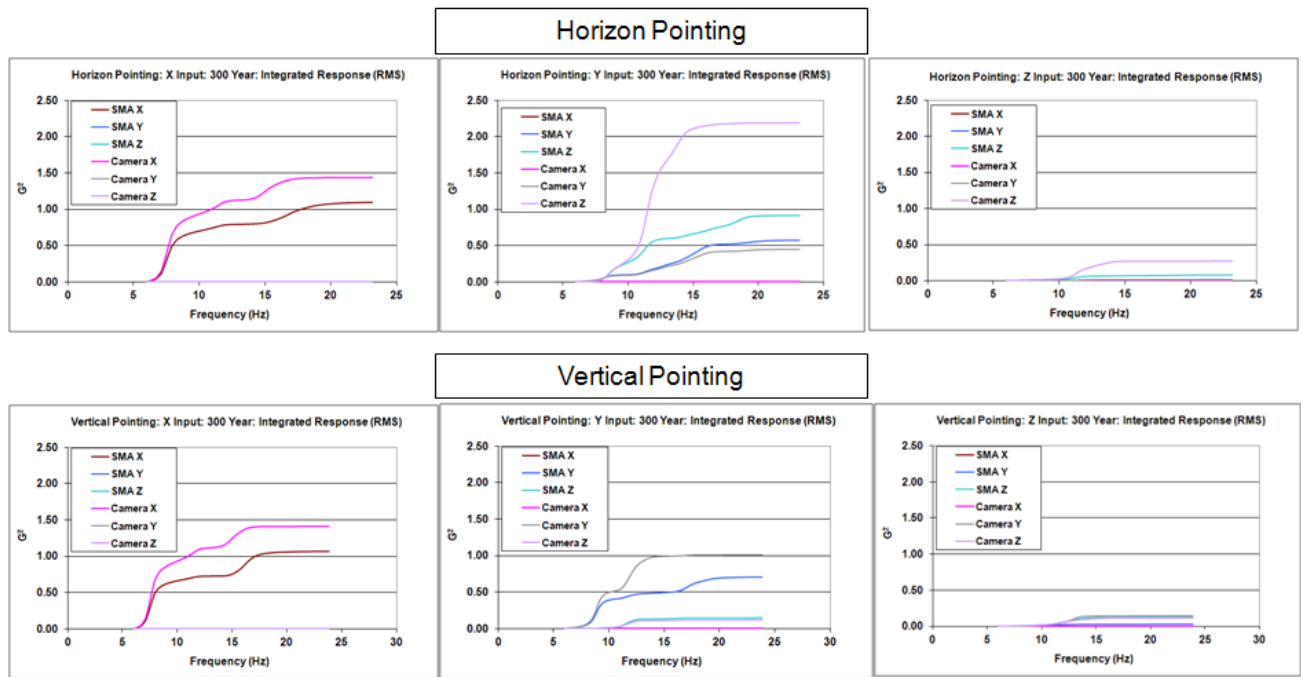


Figure 12. Integration of Output PSD.

Table 1. Seismic Accelerations Produced by X, Y and Z input PSDs.

Horizon Pointing: Horizontal X Seismic Input: Response (G)							Vertical Pointing: Horizontal X Seismic Input: Response (G)						
Return	Secondary Mirror Assembly			Camera			Return	Secondary Mirror Assembly			Camera		
Period	X	Y	Z	X	Y	Z	Period	X	Y	Z	X	Y	Z
(years)	x	z	y	x	z	y	(Years)	x	y	z	x	y	z
300	3.15	0.01	0.03	3.60	0.01	0.02	300	3.09	0.02	0.01	3.56	0.01	0.01
150	2.64	0.01	0.03	3.03	0.01	0.02	150	2.60	0.02	0.01	2.99	0.01	0.01
75	1.87	0.01	0.02	2.14	0.01	0.01	75	1.84	0.01	0.01	2.12	0.01	0.01

Horizon Pointing: Horizontal Y Seismic Input: Response (G)							Vertical Pointing: Horizontal Y Seismic Input: Response (G)						
Return	Secondary Mirror Assembly			Camera			Return	Secondary Mirror Assembly			Camera		
Period	X	Y	Z	X	Y	Z	Period	X	Y	Z	X	Y	Z
(years)	x	z	y	x	z	y	(Years)	x	y	z	x	y	z
300	0.16	2.27	2.87	0.09	2.02	4.44	300	0.02	2.52	1.15	0.01	3.01	1.04
150	0.14	1.91	2.42	0.08	1.69	3.73	150	0.01	2.12	0.96	0.01	2.53	0.88
75	0.10	1.35	1.71	0.05	1.20	2.64	75	0.01	1.50	0.68	0.01	1.79	0.62

Horizon Pointing: Vertical Z Seismic Input: Response (G)							Vertical Pointing: Vertical Z Seismic Input: Response (G)						
Return	Secondary Mirror Assembly			Camera			Return	Secondary Mirror Assembly			Camera		
Period	X	Y	Z	X	Y	Z	Period	X	Y	Z	X	Y	Z
(years)	x	z	y	x	z	y	(Years)	x	y	z	x	y	z
300	0.01	0.33	0.84	0.01	0.30	1.56	300	0.01	0.51	1.11	0.01	1.14	1.01
150	0.01	0.28	0.71	0.01	0.26	1.31	150	0.01	0.43	0.93	0.01	0.96	0.85
75	0.01	0.20	0.50	0.01	0.18	0.93	75	0.01	0.30	0.66	0.00	0.68	0.60

Per the guidelines of [3], the three output accelerations (X, Y, Z) resulting from the vertical (Z) input acceleration were combined RSS (Root-Sum-Square) with either the three output accelerations resulting from an X horizontal input accelerations or the three output accelerations resulting from a Y horizontal input accelerations, table 2. The X horizontal and the Y horizontal accelerations act independently [3], and need not be combined.

Table 2. Root-Sum-Squared (RSS) Combined Horizontal and Vertical Seismic Accelerations:

Horizon Pointing: RSS Combined X and Z Seismic Accelerations (G)							Vertical Pointing: RSS Combined X and Z Seismic Accelerations (G):						
Return	Secondary Mirror Assembly			Camera			Return	Secondary Mirror Assembly			Camera		
Period	X	Y	Z	X	Y	Z	Period	X	Y	Z	X	Y	Z
(years)	x	z	y	x	z	y	(Years)	x	y	z	x	y	z
300	3.15	0.33	0.84	3.60	0.30	1.56	300	3.09	0.51	1.11	3.56	1.14	1.01
150	2.64	0.28	0.71	3.03	0.26	1.31	150	2.60	0.43	0.93	2.99	0.96	0.85
75	1.87	0.20	0.50	2.14	0.18	0.93	75	1.84	0.30	0.66	2.12	0.68	0.60

Horizon Pointing: RSS Combined Y and Z Seismic Accelerations (G)							Vertical Pointing: RSS Combined Y and Z Seismic Accelerations (G)						
Return	Secondary Mirror Assembly			Camera			Return	Secondary Mirror Assembly			Camera		
Period	X	Y	Z	X	Y	Z	Period	X	Y	Z	X	Y	Z
(years)	x	z	y	x	z	y	(Years)	x	y	z	x	y	z
300	0.16	2.29	2.99	0.09	2.04	4.70	300	0.02	2.57	1.60	0.02	3.22	1.45
150	0.14	1.93	2.52	0.08	1.71	3.96	150	0.02	2.16	1.34	0.01	2.71	1.22
75	0.10	1.36	1.78	0.05	1.21	2.80	75	0.01	1.53	0.95	0.01	1.91	0.86

The principal purpose of this investigation is to determine the design accelerations for the LSST secondary mirror and camera. Since they are attached to the telescope's elevation assembly, the orientation of their coordinate system (x,y,z) relative to the azimuth coordinate system (X,Y,Z) varies with zenith angle, figure 8. When the telescope is zenith pointing the two coordinate systems align,  $x = X$ ,  $y = Y$ ,  $z = Z$ . When the telescope is horizon pointing the two system are related by  $x = X$ ,  $y = Z$  and  $z = -Y$ . Since the response PSD represent sinusoidal accelerations, the negative sign in front of the Y value can be ignored. The components must be designed to withstand the maximum loading which is a combination of seismic and gravitational acceleration. Consequently, the gravitational and seismic accelerations were combined, table 3.

Table 3. Combined Gravitational and Seismic Accelerations:

Horizon Pointing: Combined X and Z Seismic Accelerations With Gravity (G)										
Return	Secondary Mirror Assembly					Camera				
Period	X	Y	Z	X	Y	Z	X	Y	Z	
(years)	x	+z	-z	+y	-y	x	+z	-z	+y	-y
300	3.15	0.33	0.33	-0.16	1.84	3.60	0.30	0.30	0.56	2.56
150	2.64	0.28	0.28	-0.29	1.71	3.03	0.26	0.26	0.31	2.31
75	1.87	0.20	0.20	-0.50	1.50	2.14	0.18	0.18	-0.07	1.93

Vertical Pointing: Combined X and Z Seismic Accelerations With Gravity (G)										
Return	Secondary Mirror Assembly					Camera				
Period	X	Y	Z	X	Y	Z	X	Y	Z	
(Years)	x	+y	-y	+z	-z	x	+y	-y	+z	-z
300	3.09	0.51	0.51	0.11	2.11	3.56	1.14	1.14	0.01	2.01
150	2.60	0.43	0.43	-0.07	1.93	2.99	0.96	0.96	-0.15	1.85
75	1.84	0.30	0.30	-0.34	1.66	2.12	0.68	0.68	-0.40	1.60

Horizon Pointing: Combined Y and Z Seismic Accelerations With Gravity (G)										
Return	Secondary Mirror Assembly					Camera				
Period	X	Y	Z	X	Y	Z	X	Y	Z	
(years)	x	+z	-z	+y	-y	x	+z	-z	+y	-y
300	0.16	2.29	2.29	1.99	3.99	0.09	2.04	2.04	3.70	5.70
150	0.14	1.93	1.93	1.52	3.52	0.08	1.71	1.71	2.96	4.96
75	0.10	1.36	1.36	0.78	2.78	0.05	1.21	1.21	1.80	3.80

Vertical Pointing: Combined Y and Z Seismic Accelerations With Gravity (G)										
Return	Secondary Mirror Assembly					Camera				
Period	X	Y	Z	X	Y	Z	X	Y	Z	
(Years)	x	+y	-y	+z	-z	x	+y	-y	+z	-z
300	0.02	2.57	2.57	0.60	2.60	0.02	3.22	3.22	0.45	2.45
150	0.02	2.16	2.16	0.34	2.34	0.01	2.71	2.71	0.22	2.22
75	0.01	1.53	1.53	-0.05	1.95	0.01	1.91	1.91	-0.14	1.86

Finally, since the camera is mounted on a rotator (between the camera and hexapod), the actual design accelerations are provided in maximum transverse value. The transverse acceleration is the maximum of the  $x$  and  $y$  directions. Since it unlikely that these peak accelerations will align temporally, they should be considered separately.

Table 4. Maximum Combined and Design Accelerations:

Return	Maximum Combined Seismic and Gravitational Accelerations									
Period	Secondary Mirror Assembly					Camera				
(Years)	x	+y	-y	+z	-z	x	+y	-y	+z	-z
300	3.15	2.57	3.99	2.29	2.60	3.60	3.70	5.70	2.04	2.45
150	2.64	2.16	3.52	1.93	2.34	3.03	2.96	4.96	1.71	2.22
75	1.87	1.53	2.78	1.36	1.95	2.14	1.91	3.80	1.21	1.86

Combined Design Accelerations: Peak Seismic and Gravitational (G)								
Design	Secondary Mirror Assembly					Camera		
Level	x	+y	-y	+z	-z	t	+z	-z
Survival	3.15	2.57	3.99	2.29	2.60	5.70	2.04	2.45
Operational	2.64	2.16	3.52	1.93	2.34	3.80	1.21	1.86

Only the 300 year design PSD was applied directly to the FEA model. Since the analysis is all linear and the 150 year and 75 year input PSDs were determined from scaling [1] from the 300 year PSD, the equivalent output PSDs were also determined by direct scaling.

## 6. CLOSED FORM VERIFICATION

The results determined by the previous FEA analysis can be verified by closed form (CF) methods, figure 13. Although this analysis method is principally closed form, the natural frequencies determined by FEA model for the telescope and camera must still be utilized in the amplification equations. The single resonator amplification  $\{A(f)\}$  provided previously can be utilized to directly determine the response of the telescope. As discussed earlier, the square of the amplification is combined with the input PSD to determine the output PSD. The output PSD is then integrated over the frequency to determine the RMS acceleration. The peak acceleration is then three times this value.

The camera (or secondary mirror assembly) does not directly experience the input (ground) PSD. It instead experiences the motions of the telescope, figure 13. By combining the amplification (as a function of frequency) of the telescope with the amplification of the camera, the coupled amplification between the ground and the camera can be determined. The coupled implication is then combined with the input PSD to determine the output PSD which is then integrated to determine the RSS and peak values.

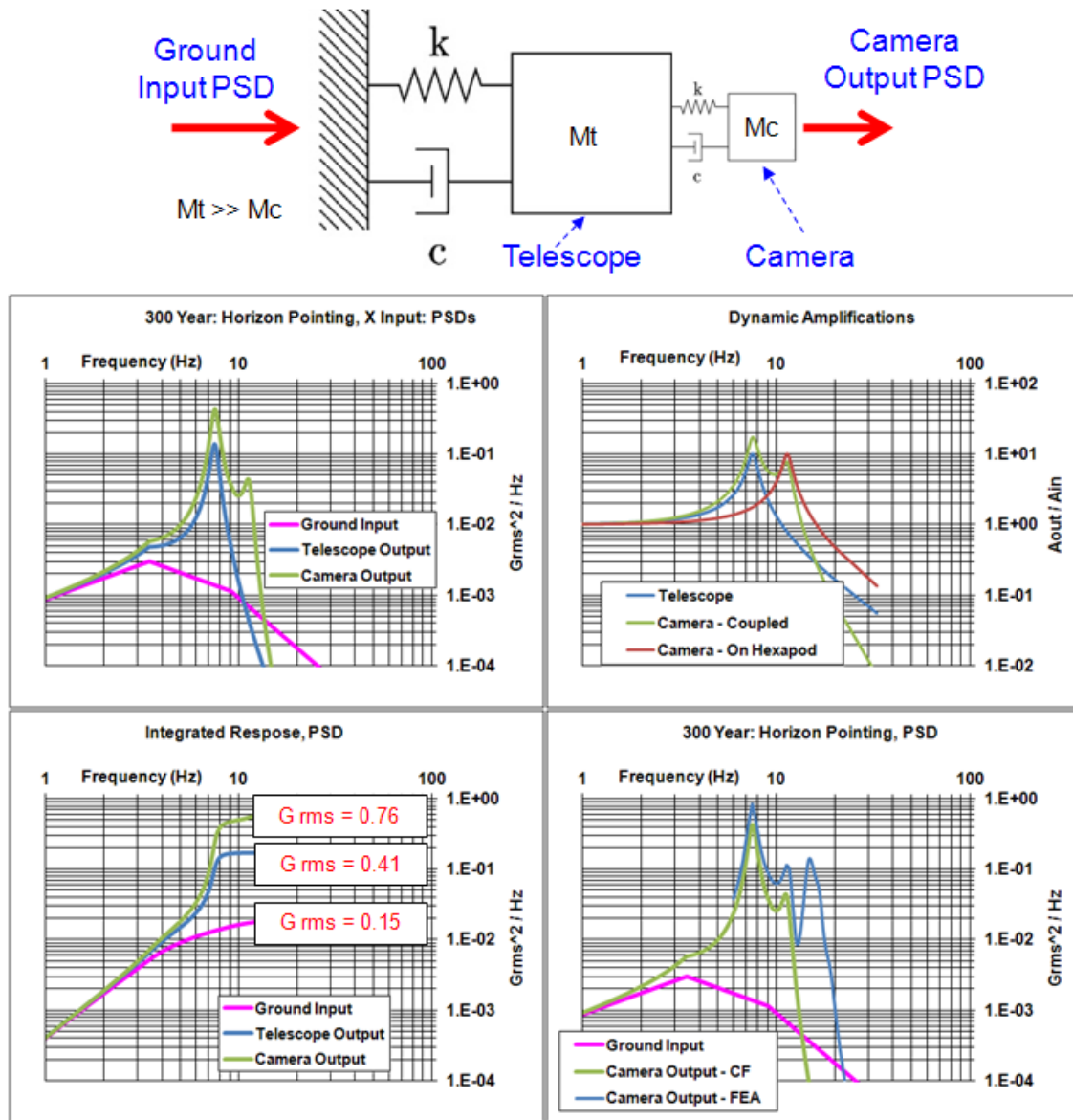


Figure 13. Closed form verification of analysis

The result of this closed form analysis were compared to the initial PSA and the FEA, table 5. The closed form values for peak ground acceleration and telescope acceleration were essentially identical to the initial PSA values. The FEA determined acceleration of the camera of 3.6 G is 60% higher than the 2.28 G value provided by this closed form analysis. Some of this variation is the result of the CF analysis not accounting for the flexibility between the CG of the telescope, which is on the elevation axis, and the mounting location of the hexapod flange. More importantly, an examination of the FEA output PSD, figure 13 lower right, reveals that two vibration frequencies are participating in the vibration coupling. The CF analysis only considered the camera natural frequency at 11.37 Hz. A second natural frequency of 14.92 Hz is adding substantial motion to the system and increasing the total acceleration.

Table 5. Closed Form Analysis Verification Table, Accelerations in G:

Comparison of 300 Year Accelerations Horizon Pointing: X Acceleration				
5% Damp	RMS	Peak Values		
	CF	CF	PSA	FEA
Ground	0.15	0.44	0.45	na
Telescope	0.41	1.24	1.22	na
Camera	0.76	2.28	na	3.6

The general agreement between the CF analysis, the PSA and the FEA verifies the analysis. The increase in the FEA determined accelerations (3.60 G) over the closed form values (2.28 G) demonstrates the limitations of the closed form method. Not only does the FEA provide large accelerations, but these larger accelerations are explainable by the FEA output PSD.

## 7. DAMPING EFFECTS

All the previous analysis assumed 5% damping. Although this value is commonly used for buildings it is excessive for telescopes without added damping. Telescope operations require minimal hysteresis. Minimizing hysteresis inherently minimizes damping. Preliminary measurements at the SOAR telescope imply approximately 2% natural damping which is congruent with [3] which recommends damping levels of 2-3% for similar structures.

Meeting the LSST's stringent slew and settling specifications requires added damping. This added damping is in both the financial and mass budgets. Requiring the damping units to function to up to the seismic event level is significantly more demanding than only requiring operational level damping. Consequently, the analysis was repeated for the closed form verification case (horizon pointing X input acceleration) and for the alternative damping level of 2%.

According to [1] the peak accelerations should vary with the inverse square root of the damping level. Consequently, reducing the damping from 5% to 2% should produce a 58% increase in the peak accelerations. (Square root (5/2) = 1.58). As shown in table 6 and figure 14, reducing the damping from 5% to 2% produced a slightly greater increase than this theoretical 58% increase (60% increase in closed form analysis, 73% increase for FEA analysis). Producing a secondary mirror cell assembly and camera assembly which could survive the accelerations resulting from 2% damping would be very difficult. Consequently, the utilization of added damping to reduce the seismic accelerations for the LSST telescope is necessary.

Table 6. Results For 2% Damping, Accelerations in G:

Comparison of 300 Year Accelerations Horizon Pointing: X Acceleration			
2% Damp	RMS	Peak Values	
	CF	CF	FEA
Ground	0.15	0.44	na
Telescope	0.65	1.94	na
Camera	1.22	3.66	6.26
Cam % Increase	60%	60%	74%

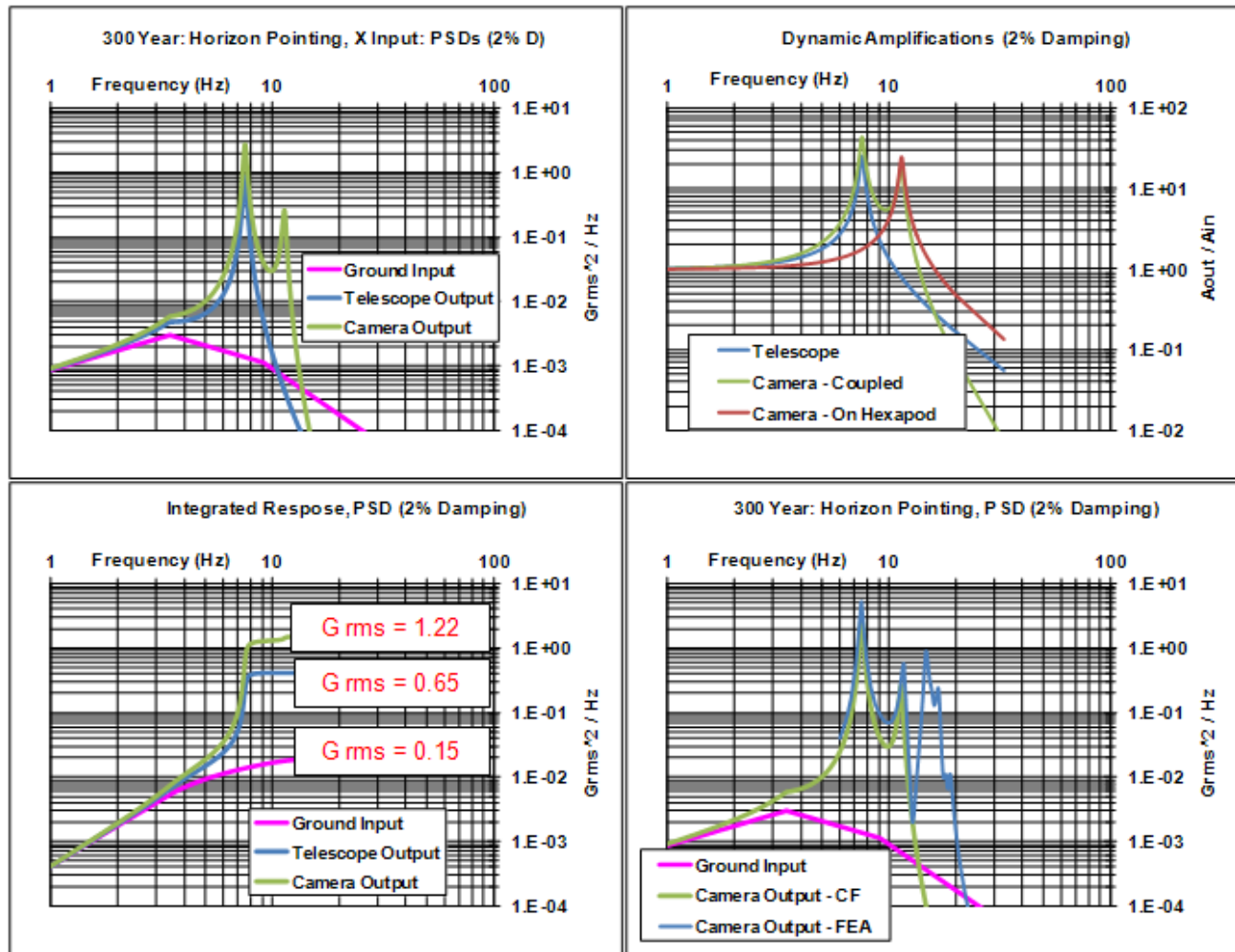


Figure 14. Closed form analysis with 2% damping.

## 8. SUMMARY

To determine the seismically induced accelerations of the LSST secondary mirror assembly and camera, a comprehensive finite element model of the telescope, its pier and mountain top was developed and analyzed according to the guidelines of the Chilean Standards (Norma Chilena). An input PSD based on [1,2] and corresponding to a 300 year return period was applied to the FEA model and the resulting accelerations of the secondary mirror and camera were determined. The accelerations for 150 year and 75 year events were determined from the 300 year event by scaling.

Since the analysis method determines the total acceleration by integrating over the output PSD, it assumes all the vibration frequencies are excited simultaneously and indefinitely. Consequently the methodology is inherently significantly conservative. Although the resulting accelerations are rather large, since the analysis method is inherently conservative, significant factors of safety need not be applied to these accelerations.

The analysis assumes 5% damping which is large for a typical large ground based telescope. However, the LSST telescope must incorporate added damping to meet its stringent slew and settling time requirements. Without this added damping, the telescope would experience significantly larger accelerations.



## 9. REFERENCES

- [1] Neill, D. R., Warner, M., Sebag, J., "Seismic Design Accelerations for the LSST Telescope," SPIE 8444-113, (2012).
- [2] Chilean Standard, "Earthquake-resistant design of base-isolated buildings: Análisis y Diseño de Edificios con Aislación Sísmica," Instituto Nacional de Normalización, NCh2745-2003, (2003).
- [3] Chilean Standard, "Seismic design of industrial structures and facilities: Diseño Sísmico de Estructuras e Instalaciones Industriales," Instituto Nacional de Normalización, NCh2369-2003, (2003).
- [4] Chilean Standard, " Earthquake resistant design of buildings: Diseño Sísmico de Edificios," Instituto Nacional de Normalización, NCh 433-1996, (2009).
- [5] Steinberg, D., [Vibration Analysis for Electronic Equipment, 3<sup>rd</sup> Addition,] A Wiley Inter-science Publication, ISBN 0-471-37685-X, (2000).
- [6] Anderson, E. H., Glaese R. M. and Neill, D. R., "A comparison of vibration damping methods for ground based telescopes," SPIE 7012, (2008).